Annals of the Academy of Romanian Scientists
Series on Physics and Chemistry Sciences
ISSN 2559-1061 Volume 2, Number 1/2017

FORECASTING OF ENERGY PRODUCTION AND OPERATIONAL OPTIMIZATION FOR PHOTOVOLTAIC SYSTEMS

Laurentiu FARA,[1,2] Alexandru DIACONU,[1]Dan CRĂCIUNESCU[1]

Rezumat. *In order to forecast the solar radiation, two statistical models, namely Artificial Neural Network (ANN) and Autoregressive Integrated Moving Average (ARIMA), were analyzed. Considering these methods, an estimation of energy production for BIPV systems and PV parks as well was developed. The results obtained by ANN and ARIMA models for the analyzed case studies were compared between them. We analyzed the fluctuations of daily solar irradiation and defined a few synoptic situations to include the cloudiness changes. In this way it is possible to improve the forecasting quality. The solar radiation forecasting based on the two statistical models could be applied with good results on short term and long term as well. Based on complete data sets that include meteorological parameters, such as: 1) air temperature 2) cloudiness, 3) atmospheric pressure, 4) relative humidity and 5) sunshine duration as input data, we minimized the forecasting errors and achieved a more accurate estimation of the power output for the studied PV park.*

Taking into account this approach regarding the forecasting of the PV systems, we could introduce a short analysis of the PV market development using the worldwide PV market performances and features for 2014. The European PV market pointing on its prospects and forecasts until 2019 was characterized.

Keywords: forecasting, solar radiation, statistical models, variability index, energy production, BIPV system, PV Park, PV market

1. INTRODUCTION

In the past few years, the percentage of energy obtained from renewable energy sources has increased considerably. This type of energy presents numerous advantages, leading to the sustainable development of the society but has a major disadvantage: it is very fluctuant. This disadvantage becomes more and more an issue, as the overall percentage of renewable energy increases, having a negative impact on the energy distribution equipments as well as on the energy quality.
In order to obtain a high penetration rate of PV systems **[1]**, two challenges have to be considered: 1) variability (the PV output has a variability at all timescales) and 2) uncertainty (the variability is difficult to be predicted).

The two main features characterising the strong dissemination of PV systems are represented by: 1) variability, and 2) uncertainty **[2].** Due to its variability, PV output has fluctuations at all timescales (from seconds to years), while the

[1]University ”Politechnica” of Bucharest (Romania).
[2]Academy of Romanian Scientists, Bucharest (Romania).

uncertainty determines difficulties for output forecasting. The forecast could be applied to one PV system or to several PV systems distributed on a specific geographical area. The forecasts could aim on output power of PV systems or on its rate of change (ramp rate), **[3].** Forecasting methods could be based on different tools and databases, supplied by weather stations, satellites or outputs obtained from numerical weather prediction models (NWP), **[4].** The main weather forecasting parameters are: global horizontal irradiance and ambient temperature. The main forecasting models could be defined as physical and statistical ones. Our article is focused on two statistical models, namely Autoregressive Integrated Moving Average (ARIMA) and Artificial Neural Network (ANN), **[5, 6, 7].** The statistical approach depends on past data to "train" models without dependence on PV models.

There are two classes of forecasting methods developed for different forecast horizons, **[8]**:

- intra-day forecasts (PV forecasting from 0 to 6 hours). For instance, NWP models could be applied for intra-day forecasts.
- PV forecasting from 6 hours to multiple days.

Specific point has to be addressed to forecast accuracy. There were several attempts to improve solar forecast standardizing **[9].** Common metrics proposed include mean absolute error (MAE), mean bias error (MBE) and root mean quadratic error (rMSE) **[10].**

Considering electric PV energy, obtained through small PV systems or large photovoltaic power plants, it varies not only on annual cycles (different incident angles of the solar radiation depending on the season) or daily cycle (day and night cycle) but also depend on spontaneous factors such as cloudiness, nebulosity, and aerosol content **[11].**

The forecast precision is influenced by the following aspects: regional climate, meteorological conditions, forecast horizon and precision metrics.

The article tried to concentrate some of these ideas on specific case-studies: a BIPV system (located at Renewable Energy Lab, Faculty of Applied Sciences, Polytechnic University of Bucharest) **[12]** and a PV park, located in the southern part of Romania, **[13].** The forecasting of energy production for PV systems/ Parks could contribute to their exploitations in the best conditions what could determine to an improvement/optimization of the operational efficiency of these units. The forecasting approach of PV systems is extremely useful to understand the PV market on local, European or worldwide level, **[14].** Some features of the PV market development on European and world level are analyzed in this review article.

2. SOLAR RADIATON FORECASTING BASED ON TWO STATISTICAL MODELS: ARIMA AND ANN

2.1 Preliminary

In the recent years, the energy quota production from **R**enewable **E**nergy **S**ources (RES) has grown considerably. This renewable energy presents numerous advantages, which lead to the sustainable development of society, but it has a major disadvantage: it is very fluctuant. This disadvantage becomes more and more an issue, because an increase in the percentage of total energy production using renewable energy sources will have a negative impact on energy distribution equipment, as well as on the quality of energy.

There are significant research efforts around the world to develop a precise forecast models in order to meet the new requirements. Incoming solar radiation depends very much on the current state of the atmosphere, weather (e.g. clouds, aerosols, etc.). Because these parameters are determined by atmospheric processes at local level, solar radiation forecasts require methods able to include physics of these processes.

In the solar radiation forecasting on short-term different approaches have been introduced using: 1) time series empirical models by Reikard, **[15],** Behrang **[16];** 2) physical models by Lara-Fangeo, **[17]** et al. and Breitkreuz et al., **[18]**; 3) satellite models by Perez et al., **[19]** Lorenz et al. **[20]** and Heinemann et al., **[21],** and 4) a combination of these models by Fernandez-Jimenez et al., **[22]** and Kratzenberg, et al., **[23]**

In the choosing of one of these models, usually are taken into account: the availability of meteorological data used as input data of the model and the precision of the model, as well. The results show that the accuracy of the forecast depends very much on the daily variability of solar irradiance. Thus, we will look at two methods that will be used in the forecast of solar radiation.

2.2 Presentation and discussion of the ARIMA (Autoregressive Integrated Moving Average) model.

The statistical ARIMA model is characterized by three parameters: p, d and q. The identifying of the correct temporal series is a process to find the values of these parameters in a way that will establish the pattern found from used data. When the value of a parameter is null, it means that the model will not be necessary.

The *d* item is identified before the *p* and *q* items. The aim is to identify if the process is stationary. Otherwise, it should be done stationary before the identifying of the *p* and *q* values.

The three terms that will be identified in the ARIMA model are:

- The autoregressive-term – *p*
- The integration term (or tendency) – *d*
- The mobile average-term – *q*

The autoregressive term determine dependences between consecutive observations. Every single term posesses an associated correlation coefficient which describes the dependency magnitude, i.e. in a model posessing two autoregressive terms *(p=2)*, an observation depends (or is forecasted) on other two observations. The mobile average-term *q* describes the endurance of a random shock (or accidental deviation) from one observation to the consecutive one. For example, in a model having *q=2*, an observation is depending on two random shocks. The integration term is intended to transform a nonstationary temporal series, into a stationary one. A model with the integration term *d=2* must be differentiated twice in order to make it stationary. Differentiation in statistics refers to a transformation applied to a data set to make it stationary.

This can be achieved if the average time series is constant (i.e. observations should fluctuate around the mean) and the variant of the series must be constant. A series is stationary if a shock is absorbed in time. If the series is not stationary, through differentiation it is necessary to reach to a stationary one; the integration order represents the number of successive required differentiations for obtaining stationary series (in general, its value is 1 or 2).

The analysis of time series is generally performed using computing machines. The main reference for ARIMA models is the ARIMA Box Jenkins, that is non – season model. In this model three stages are used to identify the process correctly:

- Model selection is done by identifying if the model would be stationary
- Estimation of parameters uses computational algorithms to determine the coefficients that describe the best model of ARIMA. The most used algorithm is represented by estimation of mean quadratic errors.
- Checking of the model is performed by testing if the selected model is specified by a stationary univariate process. If this does not happen, the process must be replayed starting with the first stage to improve the model.

An ARIMA model of type (p, q) can be described as follows, **[24]**:

$$Y_t = a_0 + a_1 Y_{t-1} + \ldots + a_p Y_{t-p} - b_1 \varepsilon_{t-1} - b_2 \varepsilon_{t-2} - \ldots - b_q \varepsilon_{t-q} \quad (2.1)$$

where *p* represents the order of autoregressive, *q* is the order of mobile average and ε_t is a white noise.

When *q = 0* we obtain the autoregressive model of *p* order, noted AR (p):

$$Y_t = a_0 + a_1 Y_{t-1} + \ldots + a_p Y_{t-p} \quad (2.2)$$

For: $p = 0$, we can get the mobile average model of order q:

$$Y_t = a_0 - b_1\varepsilon_{t-1} - b_2\varepsilon_{t-2} - \ldots - b_q\varepsilon_{t-q} + \varepsilon_t \quad (2.3)$$

2.3 Presentation and discussion of the ANN (Artificial Neural Network) model

An artificial neural network represents a calculation method that trys to imitate the operation of a human brain. An artificial neuron is a computational model inspired by natural neurons. It is known that neurons receive signals through synapses located in dendrites or neuron membrane, as can be seen in Figure 2.1. When the received signal is enough strong (it has the power to pass a certain threshold), the neuron becomes active and sends a signal to the axon. The signal may also be sent to other synapses or can activate other neurons.

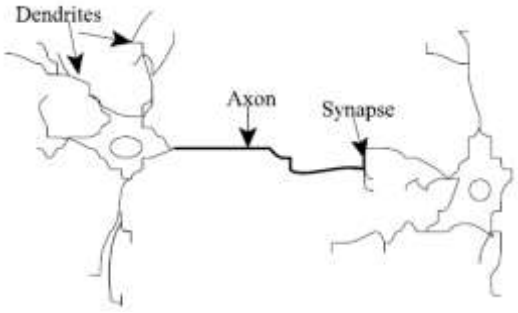

Figure 2.1: Natural Neurons (artistic concept)

The neuronal network is made of input data (proper synapses) which are multiplied by the weights and then are calculated by a mathematical function that determines the neuron activation, **[25].** A different function calculates the output of an artificial neuron that presents a dependence of certain threshold. Artificial neural networks, shown in Figure 2.2 combines artificial neurons to process information.

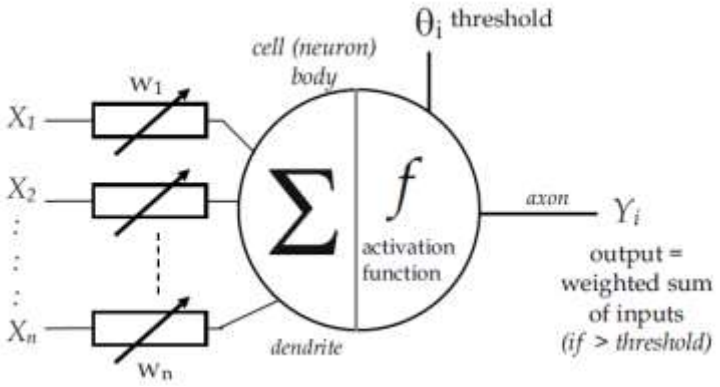

Figure 2.2: An artificial neuron

The more artificial neuron weigh is greater, the more the input multiplied by this will be stronger. By adjusting the weights, we can get the desired output for specific inputs. When in the neuronal network there are hundreds or thousands of neurons, algorithms that adjust the weights of the neural networks must be find; this process represents the training or learning of the neuronal network. The first model of neuronal network was developed by McCulloch and Pitts, **[26]** and represents a network of interconnected cells, each in functional connection with the following. Hundreds of different models of neuronal networks were developed; the major differences being are given by the used functions, learning algorithms, etc. The neuronal network model used was developed by Rumelhart and McClelland in 1986, **[27]**.

The backpropagation of errors training algorithm is based of the model developed by Rumelhart and McClelland and implements a supervised training method of a multilayer network of continuous perceptrons. This model is used in networks of feed-forward type that is the artificial neurons are organized into layers and are sending the signal forward, while errors are propagated back. The supervised training represents the fact that the network receives the algorithm with inputs and outputs would be achieved by the network and then, the errors (differences between the measured and the forecasted values) would be calculated. The goal of this algorithm is to minimize the errors so the network to learn from the data provided for training.

The activation function of artificial neurons from the neuronal network through the back-propagation algorithm is a sum of the inputs multiplied with the associated weights.

$$A_j(\bar{x}, \bar{w}) = \sum_{i=0}^{n} x_i w_{ji} \tag{2.4}$$

where, x_i represent the inputs and w_{ji} represent their weights. We can deduce that the activation of the neuron is influenced only by these inputs and their weights. If the output results in the neuron activation, then the neuron becomes linear. The most common output function is the sigmoidal:

$$O_j(\bar{x}, \bar{w}) = \frac{1}{1+e^{A_i(\bar{x},\bar{w})}} \tag{2.5}$$

The value of the sigmoidal function is very close to 1 for high positive numbers, 0.5 for 0 and very close to 0 for negative high numbers. It provides a transition between the minimum and maximum of the neuron output (close to 0 or 1). We can see that the output depends only on activation, which depends on inputs and their weights. The training process oriented to determine the best possible output for specific inputs. Because the errors represent the differences

between the present data and desired outputs, this weights have to be changed to reduce errors.

The error function for the output of each neuron can be defined by:

$$E_j(\bar{x}, \bar{w}, d) = (O_j(\bar{x}, \bar{w}) - d_j)^2 \tag{2.6}$$

It will take the quadratic of the difference between output and the target because it will always be positive and the difference will always be very big or very small. Neuronal network error will be then the sum of errors for all neurons in the output layer:

$$E(\bar{x}, \bar{w}, d) = \sum_j (O_j(\bar{x}, \bar{w}) - d_j)^2 \tag{2.7}$$

The back-propagation algorithm calculates how the errors will depend on the outputs, inputs and their weights. After this is accomplished, the adjustment of the weights can be achived by the descending gradient method:

$$\Delta w_{ji} = -\eta \frac{\partial E}{\partial w_{ji}} \tag{2.8}$$

The magnitude of the adjustments will depend on η and the weights contribution in the error function.

If the weights have a hight impact on errors, the adjustments will be larger than if the weights have a smaller impact on errors. The evaluation of the derivative of *E* in relation with w_{ji} is the aim of the backpropagation algorithm. To determine this derivative, firstly you should identifiy the dependence of the output error, what means to do the derivative of *E* in relation with O_j:

$$\frac{\partial E}{\partial O_j} = 2(O_j - d_j) \tag{2.9}$$

We could do the derivative of $O_j$in relation with w_{ji} and will obtain:

$$\frac{\partial O_j}{\partial w_{ji}} = \frac{\partial O_j}{\partial A_j} \frac{\partial A_j}{\partial w_{ji}} = O_j(1 - O_j)x_i \tag{2.10}$$

At the end we will have by combining eqs. (2.9) and (2.10):

$$\frac{\partial E}{\partial w_{ji}} = \frac{\partial E}{\partial O_j} \frac{\partial O_j}{\partial w_{ji}} = 2((O_j - d_j)O_j(1 - O_j)x_i \tag{2.11}$$

Thus, the adjustments of each weight will be:

$$\Delta w_{ji} = -2\eta(O_j - d_j)O_j(1 - O_j)x_i \tag{2.12}$$

We can use the last equation to train a neuronal network with two layers. If we would like to adapt the weights (called v_{ik}) of a previous layer, we have to calculate the dependence of errors on the inputs of this layer. For that, we could change x_i with w_{ji} in the last three equations. At the same time, we have to identify the dependence of the error for the adjustment network v_{ik}:

$$\Delta v_{ik} = -\eta \frac{\partial E}{\partial v_{ik}} = -\eta \frac{\partial E}{\partial x_i} \frac{\partial x_i}{\partial v_{ik}} \tag{2.13}$$

where

$$\frac{\partial E}{\partial w_{ji}} = 2(O_j - d_j)O_j(1 - O_j)w_{ji} \quad (2.14)$$

This type of method was used in identification, modelling, optimization and forecasting of complex systems. These systems use geographic coordinates and meteorological data such as humidity, air temperature, pressure, etc. as input data for estimation of global solar iradiance **[28].**

3. ENERGY PRODUCTION FORECASTING FOR BIPV SYSTEM BASED ON ARIMA AND ANN MODELS.

3.1 Presentation of the analysed BIPV system.

The structure of the BIPV system from Solar Energy Laboratory, Faculty of Applied Sciences, University Polytechnic of Bucharest (the selected system for our study) is presented in the Figure 3.1., **[29].**

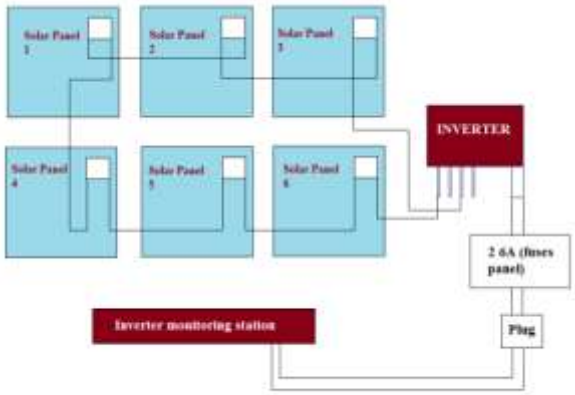

Figure 3.1: BIPV system structure (six solar panels, inverter, fuses panel, PV monitoring station and plug).

There were collected data on brightness and system performance in terms of power (Pac) for a period of five days.

Three days were used for forecast and the other two days were used for the purpose of validating of the results. In the Figure 3.2 is presented the evolution of brightnesss and power for a period of one-day in.

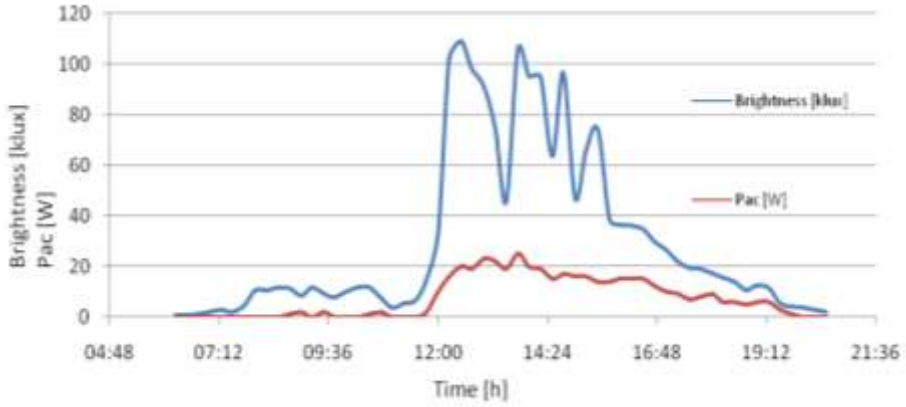

Figure 3.2: The evolution of the power (Pac) and brightness parameters on time (14.06.2012)

3.2 Energy production forecasting for a BIPV system based on ARIMA model

The comparison provides detailed data from 15 in 15 minutes, allows getting important information regarding system performance. You can notice a decrease of power in the latter part of the day.

Explication could be: 1) The PV windows is oriented towards East, so the incident solar radiation is maximum in the first part of day, 2) The system is shadowed in the second part of day.

The solar radiation data obtained using the Laboratory meteorological station, were used for the solar radiation forecasting on short term, using various methods for the location of the BIPV system. In the first phase, the ARIMA model is used.

The operation of the ARIMA model is shown in Figure 3.3. The software used for making forecasts is called IBM SPSS – is a predictive analysis software developed by IBM; it offers a range of statistical procedures including the linear regressions, Monte Carlo simulations, geospatial analysis, etc.

If the forecasting process contain seasonal fluctuations, the process becomes ARIMA (p, d, q) (P, D, Q) s, where *p* is the AR process order, *d* is the term differentiation, q is the mobile average order, P is the AR seasonal process order, Q is the MA order, D is the seasonal differentiation order and s is the length of the seasonal period.

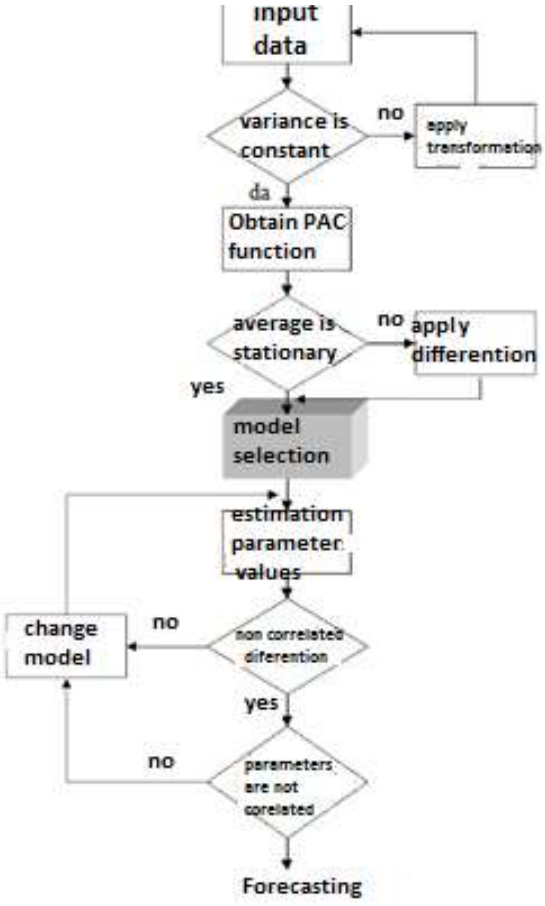

Figure 3.3: The operation of the ARIMA model
for forecasting of energy production for PV system

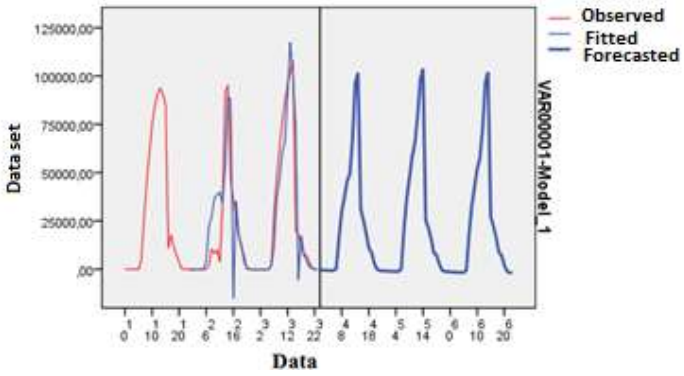

Figure 3.4: The results of ARIMA forecasting model: observed data (13-15.06.2012),
fitted data and forecasting values (16-18.06.2012)

The results of ARIMA model are represented by input data set for June 13 - 15.06, while the model is verified by data 16.06-18.06, see Figures 3.4 and 3.5. The selected model for solar radiation forecasts is of the type ARIMA (1,0,0) (1,1,0). This is due to the choice of the Akaike-Schwarz selection criterion, **[30].**

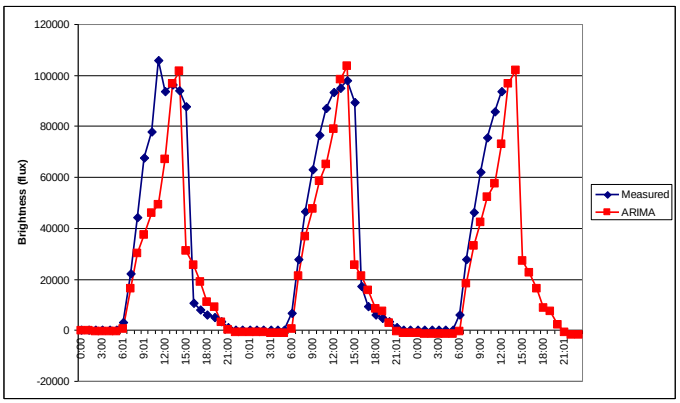

Figure 3.5: The fitting of the forecasting data for ARIMA model and measured data.

3.3 Energy production forecasting for a BIPV system based on ANN model

Two main classes of neural networks architecture can be identified, namely: the architecture based on the propagation of information from the input data to the output ones, and the architecture of feed-forward type; the second class is represented by the architecture of recurrent networks. The operation of a neural network is represented in Figure 3.6.

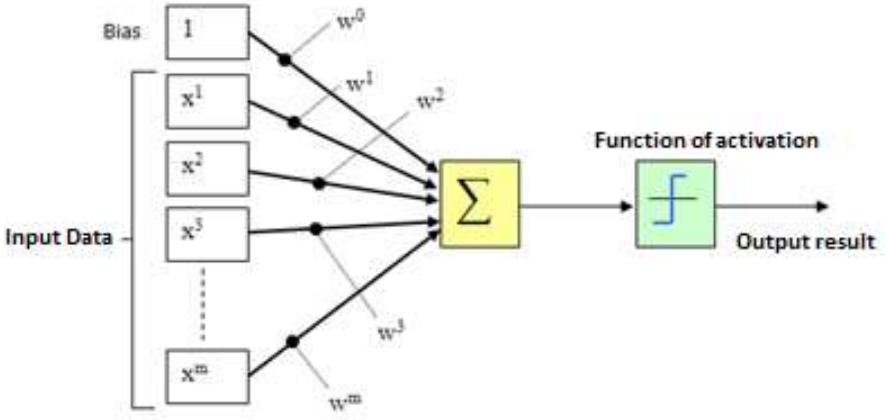

Figure 3.6: The operation of ANN model for the energy output forecasting for a PV system

Taking into account five meteorological variables, namely: air temperature, relative humidity, atmospheric pressure, wind speed and duration of sunlight brightness, was made to forecast data for 16.06.2012 using ANN model, see Figure 3.7.

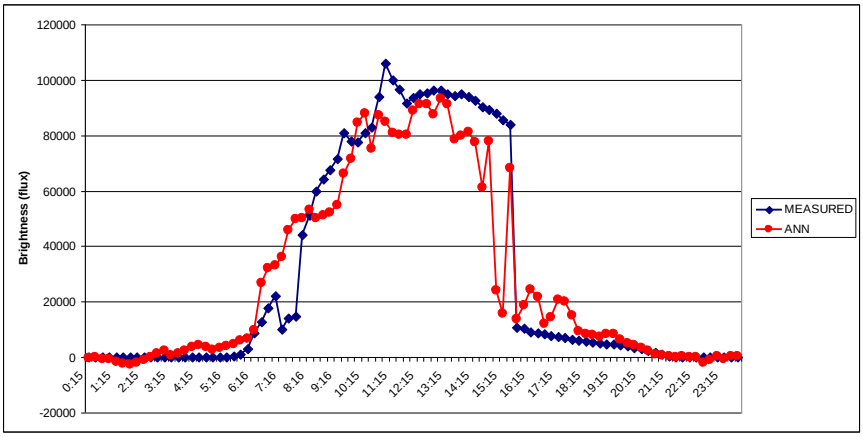

Figure: 3.7: Fitting of forecasted data using ANN model and measured data (16.06.2012)

A statistical relationship between global solar radiation and energy production is defined, taking into account the technical characteristics of the PV system, system losses and its location. Pac forecasting values were compared with the measured ones, see Figure 3.8.

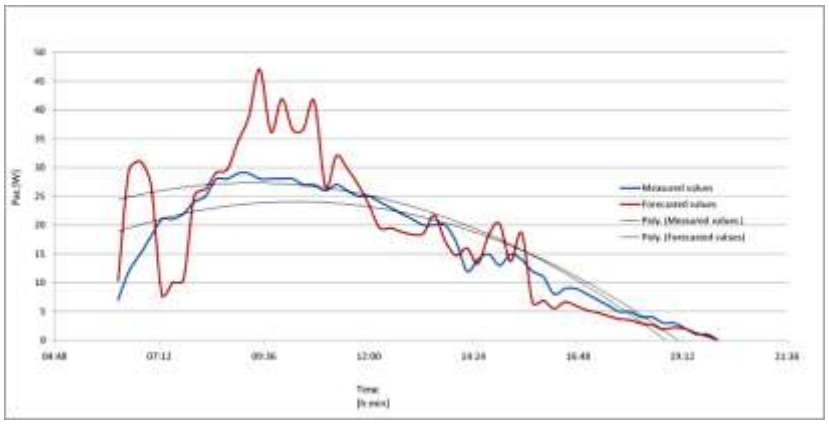

Figura 3.8 Comparison between the forecasted values and measured ones for Pac on 17.06.2012

The error between the measured and calculated forecasting values for Pac using the ANN model is 8.89%.

3.4 The improvement of forecasting quality: index of variability for solar radiation

Solar radiation forecasting error depends on the daily variation of solar radiation. At the same time, the daily fluctuation of solar radiation shows an important correlation with cloudiness, so, the information concerning cloudiness will be necessary to increase the accuracy of the forecast. In the most cases the accepted results could not be obtained.

In order to take into account the influence of the cloudiness, but reducing the number of the input data, we could introduce empirical indicator, namely:

$$V_{DR} = \frac{\sigma_{DR}}{\chi_{MR}} \tag{3.15}$$

In the eq. (3.15) we have: V_{DR} – the variability index of solar radiation, χ_{MR} – the monthly average global solar radiation, σ_{DR} – the standard error of global solar radiation.

In fact, this variability index quantifies the variation of solar irradiance in a specific day, compared with the overall situation for solar irradiance in a month; the variation of solar irradiance in previous days is taken into account indirectly by the monthly average. This daily index offers more detailed information, as a classification based on a synoptic situation.

The four situations include changes in the cloudiness on the previous day and on the forcasted day and are the following, see Figure. 3.9:

1. Situation of overcast/fog on the forecasted day and situation with partly cloudy sky/clear sky on the previous day V_{DR}< 0.5 (on the previous day V_{DR} > 0.5)
2. Situation of overcast/fog on the forecasted day and the situation with the sky overcast/fog on the previous day V_{DR} < 0.5 (on the previous day V_{DR} < 0.5)
3. Situation of the partly cloudy sky/clear sky on the forecasted day and situation with overcast/fog on the previous day V_{DR}> 0.5 (on the previous day V_{DR} < 0.5)
4. Situation of the partly cloudy sky / clear sky on the forecasted day and situation with partly cloudy sky/clear sky on the previous day V_{DR}> 0.5 (on the previous day V_{DR} > 0.5)

The accuracy of the solar irradiance forecast of developed in the four situations has been achieved using temporal series of ARIMA and ANN models in order to quantify the meaning of the forecasting error **[31, 32, 33, 34]**. Considering the frequency of situations over the investigated period, the most common situation is the fourth that represents 64% of the cases. The less common situation is the second, with a frequency of 8-11% of cases, see Figure 3.10. By this method, the errors of forecasts for daily solar radiation can be quantified even during the

forecasting process, defining only three situations, namely: 1) the situation of cloudiness; 2) the situation of fog; 3) the situation of partly cloudy sky / clear sky

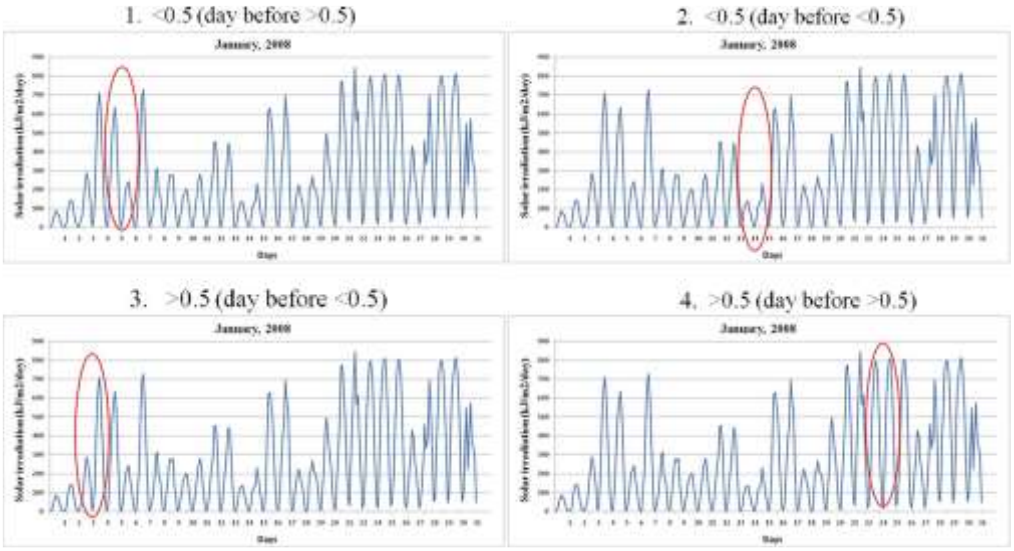

Figure 3.9: The four situations of cloudiness changes quantified by V_{DR} index, based on solar irradiance, for Bucharest/Afumati, Meteorological Station (kJ/m2/day).

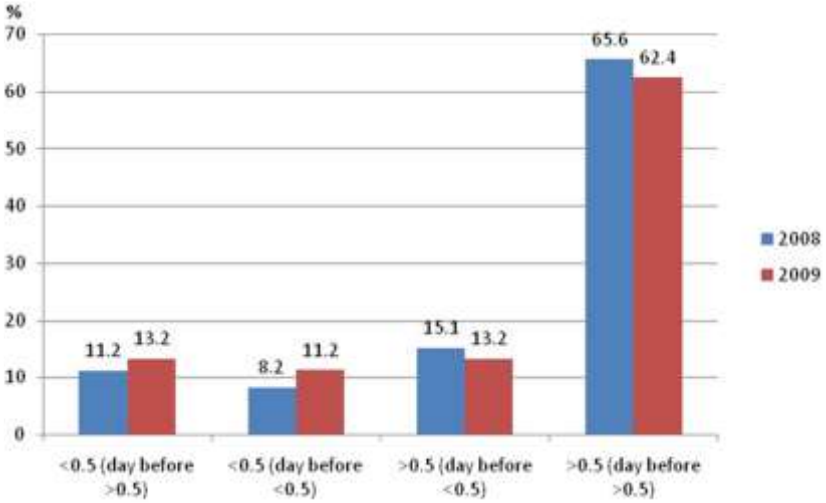

Figure 3.10: The relative frequency of the four situations of solar irradiation/cloudiness quantified by V_{DR} index, at Bucharest/Afumati Meteorological Station.

4. SOLAR RADIATION FORECASTING ON SHORT TERM AND LONG TERM

4.1 Solar forecasting on short term

Using statistical ARIMA and ANN models, short-term forecast was done taking into account the synoptic situations of quantified days by V_{DR} index **[35, 36]**. For the both models the analysed temporal series is 10 days. The accuracy of forecasts is quantified by calculation of the relative average quadratic error, using the following:

$$rRMSE = \sqrt{\frac{1}{n}\sum_{t=1}^{n}(F_t - A_t)^2} * {}^{100}/_{G_n} \quad (4.16)$$

where:F_t represents forecasting value, A_t represents the actual (measured) value, n is the number of forecasting points, G_n represents the actual (measured) average values daily.

Tables 4.1 and 4.2 include the results of the corresponding forecasts of the four situations. The best results are obtained in the case of situations of partly cloudy sky/clear sky on the forecasted day and the partly cloudy sky/ clear sky on the day previous, where monthly rRMSE varies between 6.2 and 53% while the annual one is less than 26.7%.

In the case of situations of overcast/fog on the forecasted day and overcast/fog on the previous day, as well as on in the case of situations the partly cloudy sky/clear sky on the forecast day and overcast/fog on the previous day, the accuracy of forecasts is relatively similar, ranging from 52.6% to 96.8%.

In the case of situations of overcast/fog on the forecasted day with partly cloudy sky/clear sky on the previous day forecasts show an enormous error of 250%.

Comparing the two models, ARIMA and ANN, it was noted that the magnitude of the errors is quite close in each case, but at the same time, the ARIMA model offers better results with 2,9% in the fourth case.

We believe that the accuracy of forecasts of depends closely on daily variation of solar radiation controlled by cloudiness, and the forecast of time series provides acceptable results in the case of situations with of the partly cloudy sky /clear sky on the forecasted day with partly cloudy sky/clear sky on the previous day, **[37, 38].**

Table 4.1: The rRMSE values (%) in the case of the four situations quantified by the V_{DR} index. The data are processes for 2008, the forecast period is 10 days [39].

	<0.5 (day before >0.5)		<0.5 (day before <0.5)		>0.5 (day before <0.5)		>0.5 (day before >0.5)	
Months	ARIMA	ANN	ARIMA	ANN	ARIMA	ANN	ARIMA	ANN
1	168.6	194.7	35.6	56.9	79.2	90.0	**9.2**	**15.9**
2	197.9	191.6	58.6	40.5	103.7	115.6	**9.9**	**21.8**
3	232.7	209.1	53.3	77.6	47.6	64.4	**39.4**	**42.6**
4	191.4	184.4	101.9	77.4	67.4	92.1	**22.2**	**26.3**
5	136.6	127.0	53.5	59.9	51.0	66.5	**12.9**	**17.2**
6	101.0	95.3	46.8	66.7	51.0	69.4	**16.3**	**22.9**
7	132.3	134.1	85.1	72.5	44.8	69.2	**25.6**	**36.4**
8	No case	No case	No case	No case	No case	No case	**23.8**	**20.9**
9	No case	No case	No case	No case	No case	No case	**6.9**	**10.9**
10	423.3	347.3	No case	No case	100.4	108.0	**12.4**	**32.6**
11	105.9	68.2	70.9	26.6	99.7	105.5	**30.0**	**24.5**
12	136.0	183.2	58.7	58.2	87.4	89.7	**35.6**	**48.2**
Mean	182.6	173.5	62.7	59.6	73.2	87.0	**20.4**	**26.7**

The rRMSE values (%) in the case of the four situations quantified by the V_{DR} index. The data are processes for 2009, the forecast period is 10 days [39].

	<0.5 (day before >0.5)		<0.5 (day before <0.5)		>0.5 (day before <0.5)		>0.5 (day before >0.5)	
Month	ARIMA	ANN	ARIMA	ANN	ARIMA	ANN	ARIMA	ANN
1	291.1	356.1	55.2	65.1	57.0	76.5	**25.7**	**33.3**
2	67.4	111.3	56.2	42.2	86.2	104.8	**28.9**	**18.8**
3	299.5	367.3	51.0	40.6	69.6	100.2	**26.8**	**23.8**
4	141.3	108.5	131.8	50.2	103.0	113.0	**20.8**	**17.0**
5	237.3	232.0	60.1	70.0	55.2	87.5	**9.8**	**14.0**
6	189.1	168.3	No case	No case	69.5	84.6	**15.0**	**24.2**
7	207.6	204.1	No case	No case	87.7	108.5	**21.5**	**28.8**
8	327.9	233.0	No case	No case	61.6	67.7	**6.2**	**19.3**
9	469.9	440.4	232.3	66.5	75.8	84.6	**15.0**	**29.0**
10	No case	No case	131.4	35.4	83.9	94.1	**53.4**	**20.3**
11	443.8	551.1	98.7	53.0	82.1	95.6	**16.7**	**24.0**
12	344.6	334.5	54.5	50.2	87.1	113.8	**51.4**	**33.5**
Mean	274.5	282.4	96.8	52.6	76.6	94.2	**24.3**	**23.8**

4.2 Solar forecasting on long term

It was also evaluated the decade variation of solar radiation whereas the long-term changes of solar energy have to be taken into account in applications **[40, 41]**. The linear regression model was applied for trend analysis. The anual data are are obtained from the World Centre Radiation Data **[42]** database and

represent the data corresponding to the period 1975-2006 for Bucharest meteorological station. The linear trend is significant at a level of 95% probability, thus it is identified an increase in solar radiation. The magnitude of the absolute change is 36.5 (± 2.43) J/cm2 day-1 /decade, as in Figure 4.1.

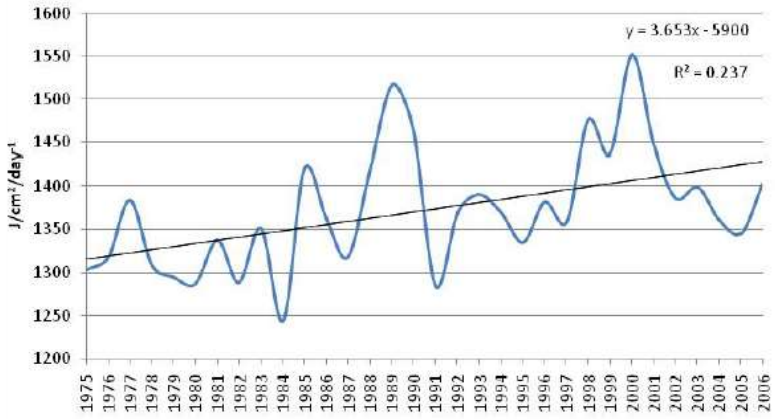

Figure 4.1 Multiannual variation of solar irradiation at Bucharest, the period of 1975-2006.

Using ARIMA and ANN forecasting models and setting the most common situation of the days in terms of weather, the solar radiation forecast has been made on January 20, 2009, as represented in Figure 4.2.

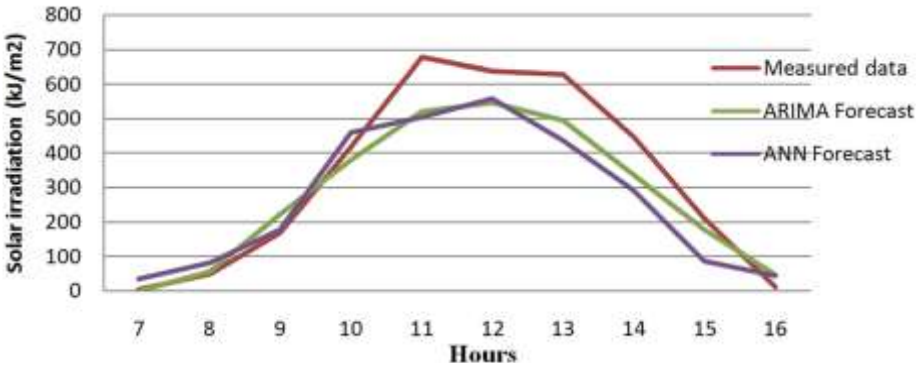

Figure 4.2: Forecast of solar irradiance for 20.01.2009 elaborated by ARIMA and ANN models.

Using this forecast, another forecast was elaborated, namely the power supplied by the BIPV system from Polytechnic University of Bucharest (PUB), shown in Figure 4.3.

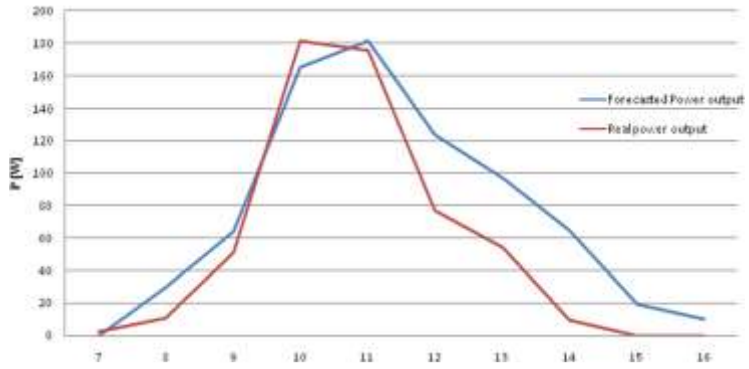

Figure 4.3: Forecasted and actual power output of the BIPV System in 20.01.2009.

In this case the calculated error was of 26.9%, and in agreement with the calculated error for the forecast of solar radiation, i.e. 26.7%. This result is due to the improving of solar radiation forecast by integrating of the data referring to different meteorological parameters (temperature, cloudiness etc.), as well as through the separation of synoptic situations depending on the variability index.

Based on the analysis of multiannual changes of solar irradiance, the forecasted power of the BIPV system for the year 2013 was evaluated, see Figure. 4.4.

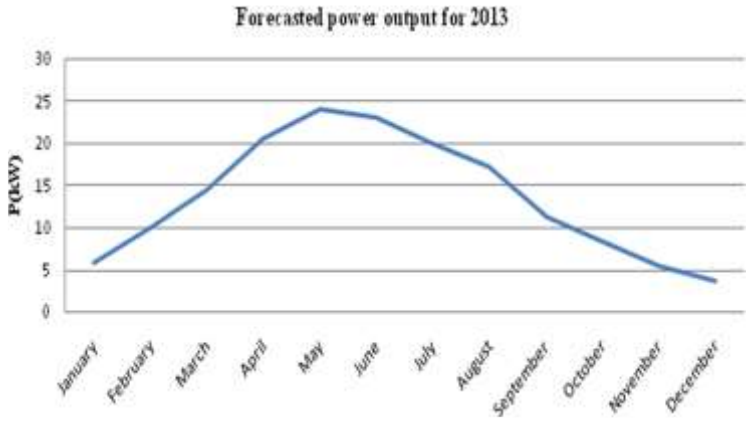

Figure 4.4: The power output of the BIPV system for year of 2013 based on the estimation of multiannual solar irradiance

It is noted that the maximum energy production of the BIPV system is carried out in May. The total forecasted energy production for 2013 is 163 kW, a result which is in line with the power performed in the previous year, respectively 157 kW.

5. ENERGY PRODUCTION FORECASTING FOR A PHOTOVOLTAIC PARK

Using the ARIMA and ANN, models we have examined the solar radiation forecast at surface (SSR), using the acquired data from analysed PV Park (in the South of Romanie). The forecasts for 10 days were developed based on previous time-series.

The forecasts have been developed for clear sky or cloudy days; in these cases the variability index of solar radiation is $V_{DR} > 0.5$. In the study period (1 July 2013-20 October 2014), the frequency of these situations is of 46.9%.

The results of the forecast conclude that the ARIMA model is more efficient than the ANN model **[43, 44, 45].** The statistics are significant in the case of ARIMA (1,0,14); this is the reason why this variant was chosen for analysis. Also, comparing the forecasted results with the measured ones,we could remark that the ARIMA (1,0,14) model is more efficient than the ARIMA (1,0,7).

The ARIMA (1,0,7) and ARIMA (1,0,14) models were selected after performing several iterations. The statistical test used to identify the most significant model is Box Ljung Statistic. In ARIMA model this test applies to residues of a fitted model not on the original series, and chek if these residues present or not autocorrelation.

The measured and forcasted values expected for August and September 2013 are presented in Figures 5.1 and 5.2.

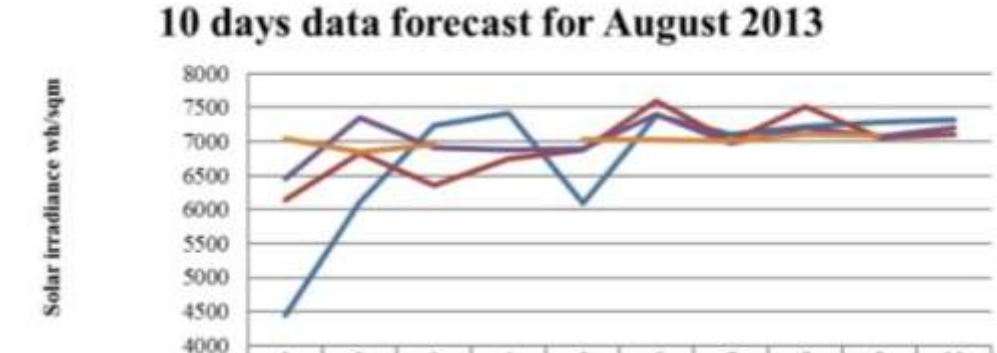

	1	2	3	4	5	6	7	8	9	10
Measured radiation	4451.3	6103.6	7240.3	7416.6	6091	7388.08	7101.34	7214.13	7285.4	7325.3
ARIMA (1,0,14)	6138.76	6822.83	6353.43	6754.42	6878.99	7598.88	7006.33	7512.72	7055.09	7109.01
ARIMA (1,0,7)	6459.48	7354.92	6916.88	6878.25	6894.17	7393.5	6974.19	7200.2	7069.23	7210.03
ANN	7044	6844	6963	no case	7024	7019	7002	7101	7098	no case

Figura 5.1 Measured and forecasted values for 10 days in August 2013, using ARIMA and ANN models

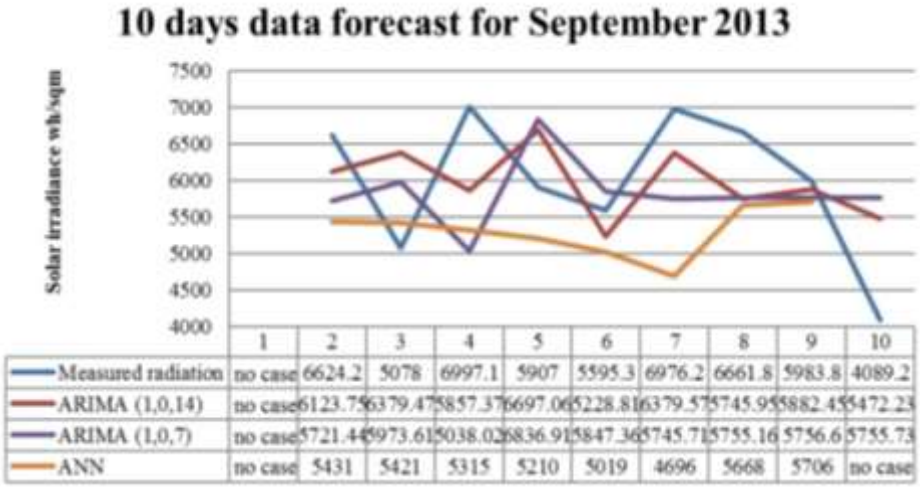

Figura 5.2 Measured and forecasted values for 10 days in September 2013, using ARIMA and ANN models

The accuracy of forecasts is quantified by the relative average absolute error (rMAE) and relative mean quadratic error (rRMSE), calculated as follows:

$$rMAE = \frac{1}{n}\sum_{i=1}^{n} |F_t - A_t| \times 100/G_n \quad (5.17)$$

$$rRMSE = \sqrt{\frac{1}{n}\sum_{i=1}^{n}(F_t - A_t)^2} \times 100/G_n \quad (5.18)$$

where: F_t represents the forecasted value, A_t reprented the measured value, n is the number of forecasted points and G_n represents the average daily irradiance of the measured values. In Tables 5.1: and 5.2: the measured and forecasted values for August and September 2013, respectively are given using ARIMA and ANN models.

Table 5.1: Measured and forecasted values for 10 days in August 2013 using ARIMA and ANN models

year	month	day	ARIMA(1.0.14) (Wh/mp)		ARIMA(1.0.7) (Wh/mp)		ANN (Wh/mp)	
			Measured	Forecasted	Measured	Forecasted	Measured	Forecasted
2013	7	31	4451.3	6138.76	4451.3	6459.48	4451.3	7044
2013	8	1	6103.6	6822.83	6103.6	7354.92	6103.6	6844
2013	8	2	7240.3	6353.43	7240.3	6916.88	7240.3	6963
2013	8	3	7416.6	6754.42	7416.6	6878.25	-	-
2013	8	4	6091	6878.99	6091	6894.17	6091	7024
2013	8	5	7388.08	7598.88	7388.08	7393.5	7388.08	7019
2013	8	6	7101.34	7006.33	7101.34	6974.19	7101.34	7002
2013	8	7	7214.13	7512.72	7214.13	7200.2	7214.13	7101
2013	8	8	7285.4	7055.09	7285.4	7069.23	7285.4	7098
2013	8	9	7325.3	7109.01	7325.3	7210.03	-	-

Table 5.2: Measured and forecasted values for 10 days in September 2013 using ARIMA and ANN models

year	month	day	ARIMA(1.0.14) (Wh/mp)		ARIMA(1.0.7) (Wh/mp)		ANN (Wh/mp)	
			Measured	Forecasted	Measured	Forecasted	Measured	Forecasted
2013	9	19						
2013	9	20	6624.2	6123.75	6624.2	5721.44	6624.2	5431
2013	9	21	5078	6379.47	5078	5973.61	5078	5421
2013	9	22	6997.1	5857.37	6997.1	5038.02	6997.1	5315
2013	9	23	5907	6697.06	5907	6836.91	5907	5210
2013	9	24	5595.3	5228.81	5595.3	5847.36	5595.3	5019
2013	9	25	6976.2	6379.57	6976.2	5745.71	6976.2	4696
2013	9	26	6661.8	5745.95	6661.8	5755.16	6661.8	5668
2013	9	27	5983.8	5882.45	5983.8	5756.6	5983.8	5706
2013	9	28	4089.2	5472.23	4089.2	5755.73	-	-

Comparison between the forecasted energy and energy given to the grid is evaluated for the period 01.08.2013-09.08.2013 for the analysed PV Park/system.

Using the collected data within the PV Park, the exported monthly energy shwous that in the period chosen for testing, respectively 01-09.08.2013, an aomunt of 513.98 MWh was inserted in the grid. The amount of solar irradiance measured in this case was of 63165.75 Wh/m^2.

We remark that: using ARIMA (1, 0, 14) model, the forecasted solar irradiance of 63091 Wh/m^2 was estimated and using ARIMA (1,0,7) model, the forcasted solar irradiance of 63891 Wh/m^2 was estimated. Taking into account the technical parameters of the PV Park/system and the forecast for solar radiation, the forecasted energy production based on the two ARIMA models will be 513.39 MWh, respectively 519.90 MWh, see Figure 5.3.

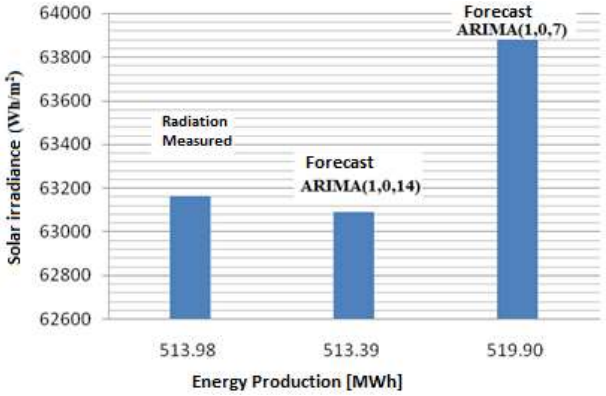

Figure 5.3: The difference between the measured values and forecasted values of solar radiation using ARIMA model

6. PV MARKET PROGRESS

6.1 Global PV Market

A. World market achievements in 2014:

On the global scale, in 2014 there were installed 40 GW of photovoltaic systems, in comparison to 38.4 GW in 2013 and 30 GW one year earlier, establishing a new record in the solar photovoltaic sector. PV, after hydroelectric power and wind energy, continues to be the third renewable energy source concerning installed capacity around the world [14, 45], thanks to PV market expansion, especially in Asia and North America.

- In Asia, the main actors are China (10.6 GW installed in 2014, feed-in tariffs measures), Japan (9.7 GW installed in 2014, feed-in tariffs measures), Korea (roughly 900 MW), Taiwan and Thailand (almost 500 MW each).
- In America, there are three countries with significant PV achievements: US (with 6.5 GW installed in 2014), Canada and Chile (with roughly 500 MW each isntalled in 2014).
- In Europe, the main installed capacities in 2014 were in the following three countries: UK (2.4 GW), Germany (1.9 GW) and France (a bit over 900 MW).
- Other world regions are represented especially by Australia and South Africa, with 900 MW installed each, in 2014.

In short, it can be remarked a significant progress, especially in Asia.

B. The global PV market characteristics in 2014 are as follows:

- *The PV contribution in the electricity mix is major*

PV and wind are the main renewable energy sources that contributed significantly to the electrical power systems in Europe. This development is stressed by the PV contribution of 6% to the peak electricity demand. For the future prospects of PV, it has to be remarked that PV will contribute more and more to the electricity mix, highlighting its integration to the grid.

- *The European PV market development speed is slowly decreasing*

Europe continues to be an important world actor in photovoltaics, based on the capacity of 88 GW installed in 2014. It is remarked an excellent balance between the utility and distribution installations in the PV market field.

- *PV systems become more and more competitive*

PV systems are characterized by two specific trends - higher performance and price decreasing - which leads to an increased competitiveness. This aspect determines the "dynamic socket parity", characterized by an increasing long-term profit, due to savings and revenues being higher than long-term financing costs.

6.2 PV market in Europe

Although the photovoltaic market on global level is characterized by a spectacular ascending trend, in Europe it is characterized by a slowing of this trend, due to reducing political support in some countries.

- The competitivity of PV systems depends not only on their technical and ecomomical performance to reduce electricity bills, but also to sell excess electricity on the markets. Several countries took retrospective measures that reduced the revenues of existing PV plants in the last few years (Spain, Czech Republic, Bulgaria and Greece), damaging the attractiveness of PV as a long-term investment.

- The main actor in the field of PV systems in Europe, namely Germany, is confronting with a small decline of PV installations, down to 3.3 GW in 2014. However, there is a total PV installed capacity in the country of 35.7 GW, although, some regulatory changes pushed the PV market down.

- It is remarkable that the 2020 targets in photovoltaics defined in 2009 have been reached by 9 countries in 2014 **[46].**

The evolution of European PV installed capacity in the period 2000-2014 is presented in Figure 6.1 **[47].** Distribution per country of annual installed capacity, cumulative installed, as well as political support for PV, is emphasized in Table 6.1 **[48].**

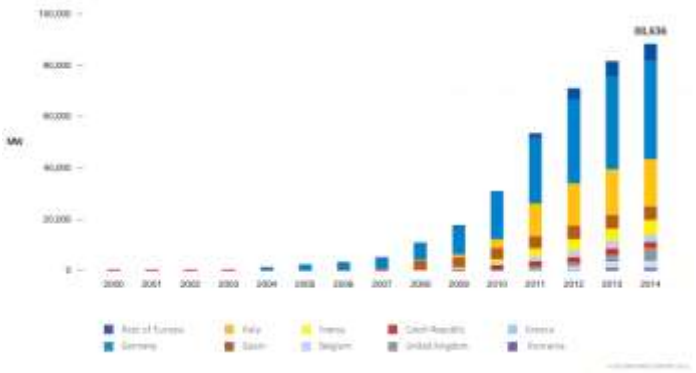

Figure 6.1 Evolution of European solar PV cumulative installed capacity 2000 – 2014 [48]

Table 6.1 Solar Photovoltaic Market and Expectations across Europe [46]

Country	Total Capacity Installed in 2014(MW DC)	Governmental support expectations
Austria	767	+++
Belgium	3.104	++
Bulgaria	1.022	+
Croatia	33	++
Denmark	608	+++
Estonia	0.2	++
Finland	11.2	+++
France	5.632	++
Germany	38.235	++
Greece	2.596	++
Hungary	80	++
Ireland	1.1	+++
Italy	18.313	++
Latvia	1.5	++
Lithuania	68	++
Luxembourg	110	+++
Malta	23	++
Netherlands	1.042	+++
Poland	34	+
Portugal	414	++

Country	Total Capacity Installed in 2014(MW DC)	Governmental support expectations
Romania	1.223	++
Slovakia	524	++
Slovenia	256	+++
Spain	5.388	+
Sweden	79	+++
Switzerland	1.046	+++
Turkey	58	+++
United Kingdom	5.230	+++

6.3 European PV market forecast until 2019

It is estimated that the solar PV market in Europe will firstly increase between 7 GW (low-case scenario) and 11 GW (high-case scenario) in 2015 before rising again in a slower manner, with installations varying between 6 GW in 2015 and 17 GW until 2019, as can be seen in Figure 6.2 **[49].**

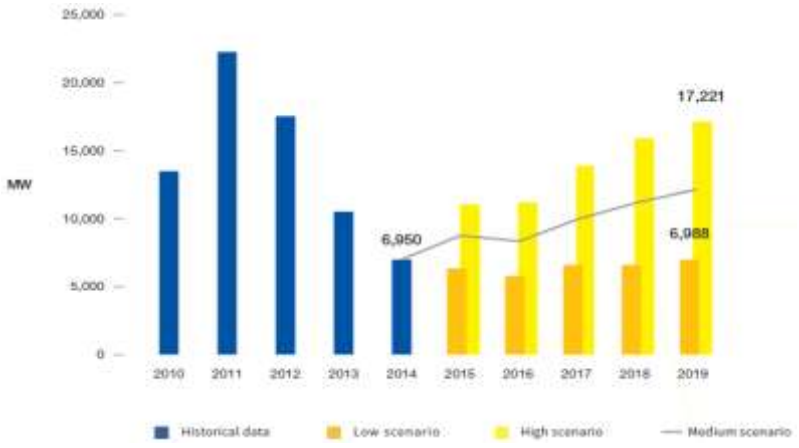

Figure 6.2: Scenarios for European solar PV market until 2019 [46]

- Considering the high-case scenario, there could be achieved a target of 158 GW installed capacity by 2019, which would represent 180% of today's PV market. The low-case scenario predicts a total installed capacity of 120 GW, while the medium scenario gives a value of 140 GW.

7. CONCLUSIONS AND PROSPECTS

7.1 Conclusions concerning forecasting of solar radiation and energy production

Solar radiation forecasts were developed in the short term using statistical models ARIMA and ANN. The efficiency of forecasted time-series is quantified by rRMSE and rMAE.

These models have been improved, separating the clear sky days and cloudy ones, using solar radiation variability index, V_{DR}. The separation of synoptic situations was performed on time series, not on forecasted values.

It was established that the most common cases for using of V_{DR} index are clear sky days in the forecasted day and in the day before, where "forecasted" day is represented by the day "tomorrow" and the day "before" is represented by "the present day" or the day when the forecast is achieved.

For the overcasted or cloudy days, these forecasting solutions offer very large errors. The forecast results have shown that the ARIMA model is more efficient than the ANN model.

The statistics are significant in the case of ARIMA (1,0,14), this is the reason why this variant was chosen for analysis. Also, comparing the forecasted results with measured values, we note that ARIMA model (1,0,14) is more efficient than ARIMA (1,0,7) The ARIMA models (1,0,7) and ARIMA (1,0,14) were selected after performing several iterations.

The statistical test used to identify the most significant model is Box Ljung Statistic. The Box-Ljung, known as the modified Box-Pierce statistic model, gives indications if a model is correctly specified.

7.2 Prospects concerning the PV Market

The PV industry is characterized now by a challenging period, with a market oriented mainly to Asia. However, Europe is the second actor in the world, although the political support decreased in many countries with great potential.
The main aspects that determine the PV market trends are:

- PV is competitive in some countries with other renewable electricity sources, based on electricity cost flattening, while in other countries the PV cost comes closer to be competitive with coonventional sources, due to an important political support.
- In the majority of countries, the PV market is characterized by a great influence of policy that determines smart and sustainable financial support platforms.

- Taking into account the huge potential of photovoltaics and its great advantages for society, the role of PV could be more and more remarkable for for the power system.
- The increasing role of photovoltaics as non-polluting, secure, cost-convenient and decentralised electricity option in the energy mix is highlighted both in Europe and all over the world.

REFERENCES

[1] R. Seguin, J. Woyak, D. Costyk, and J. Hambrick, High-Penetration PV Integration Handbook for Distribution Engineers, NREL, Technical Report, January, 2016.

[2] E. Ela, V. Diakov, E. Ibanez, and M. Heaney, Impacts of Variability and Uncertainty in Solar Photovoltaic Generation at Multiple Timescales, NREL, Technical Report, May 2013.

[3] J. Kleissl, Solar Energy Forecasting and Resource Assessment, Elsevier, 2013.

[4] J. Knievel, Numerical Weather Prediction (NWP) and the WRF Model, ATEC Forecasters Conference, July and August 2006.

[5] G. Peter Zhang, Time series forecasting using a hybrid ARIMA and neural network model, Neurocomputing 50, pp. 159 – 175, 2003.

[6] R. Huang, T. Huang, R. Gadh, Solar Generation Prediction using the ARMA Model in a Laboratory-level Micro-grid, IEEE Third International Conference of Smart Grid Communications, pp. 528-533, 5-8 November, 2012

[7] L. Fara, B. Bartok. A. G. Moraru, C. Oprea, P. Sterian, A. Diaconu, S. Fara, New results in forecasting of photovoltaic systems output based on solar radiation forecasting, Journal of Renewable Sustainable Energy 5, doi: 10.1063/1.4819301, 2013,

[8] J. Ebinnger and W. Vengara, Climate Impacts on Energy Systems: Key Issues for Energy Sector Adaptation, The World Bank Press, 2011

[9] H.G. Beyer, J. Polo Martinez, M. Suri, J.L. Torres, E. Lorenz, C. Müller, S.C. Hoyer-Klick and P. D. Ineichen, Report on Benchmarking of Radiation Products, Report under contract no. 038665 of MESoR, 2009. Available for download at http://www.mesor.net/deliverables.html, January 12, 2012.

[10] M. Shahjahan Ali, H. Rahman, S.K. Aditya and R. K. Mazumder, Accuracy Assessment of a Satellite Based Method for Solar Radiation Estimation, Dhaka Univ. J. Sci. 61(1): pp. 71-74, January, 2013

[11] E. Lorenz, J. Hurka, D. Heinemann, and H. G. Beyer, Irradiance Forecasting for the Power Prediction of Grid-Connected Photovoltaic Systems, IEEE Journal Vol. 2, no. 1, doi: 10.1109/JSTARS.2009.2020300, pp 2-10, March 2009.

[12] L. Fara, A. G. Moraru, P. Sterian, A. P. Bobei, A. Diaconu, S. Fara, Building Integrated Photovoltaic (BIPV) systems in Romania, Monitoring, modelling and experimental validation, Journal of Optoelectronics and Advanced Materials, Vol. 15, No. 1- 2, pp. 125 – 130, January – February, 2013

[13] A. Diaconu, L. Fara, B. Bartok, P. Sterian, S. Fara, Forecasting platform of PV systems based on statistical approach, Word Renewable Energy Congress, Bucharest, 8-12 June 2015.

[14] G. Masson, S. Orlandi, M. Rekinger, EPIA Global Market Outlook for Photovoltaics,2014-2018,http://www.cleanenergybusinesscouncil.com/site/resources/files/reports/EPIA_Global_Market_Outlook_for_Photovoltaics 2014-2018_-_Medium_Res.pdf

[15] G. Reikard, Predicting solar radiation at high resolutions, A comparison of time series forecasts, Solar Energy 83, pp. 342–349, 2008.

[16] M. A. Behrang, E. Assareh, A. Ghanbarzadeh, A.R. Noghrehabadi, The potential of different artificial neural network (ANN) techniques în daily global solar radiation modeling based on meteorological data, Solar Energy 84, pp. 1468–1480 , 2010

[17] V. Lara-Fanego, J. A. Ruiz-Arias, D. Pozo-Vazquez, F. J. Santos-Alamillos, and J. Tovar-Pescador, Evaluation of the WRF model solar irradiance forecasts in Andalusia (southern Spain), Solar Energy 86, pp. 2200–2217, 2012.

[18] H. Breitkreuz, M. Schroedter-Homscheidt, T. Holzer-Popp, and S. Dech, Short-range direct and diffuse irradiance forecasts for solar energy applications based on aerosol chemical transport and numerical weather modelling, J. Appl. Meteorol. Climatol 48/9, pp. 1766–1779, 2009.

[19] R. Perez, M. Kathleen, S. Wilcox, D. Renne, A. Zelenka, Forecasting solar radiation – Preliminary evaluation of an approach based upon the național forecast database, Solar Energy 81, pp. 809–812, 2007

[20] E. Lorenz, D. Heinemann, A. Hammer, Short-term Forecasting of Solar Radiation Based on Satellite Data, Proc. Eurosun (ISES Europe Solar Congress), Freiburg, Germany, 2004

[21] D. Heinemann, E. Lorenz, and M. Girodo, Forecasting of solar radiation, Solar Energy Resource Management for Electricity Generation from Local Level to Global Scale, edited by E. D. Dunlop, L. Wald and M. Suri, Nova Science Publishers, Hauppauge, 2006.

[22] L. A. Fernandez-Jimenez, A. Munoz-Jimenez, A. Falces, M. Mendoza-Villena, E. Garcia-Garrido, P. M. Lara-Santillan, E. Zorzano-Alba, and P. J. Zorzano-Santamaria, Short-term power forecasting system for photovoltaic plants, Renewable Energy 44, pp. 311–317 2012.

[23] M. G. Kratzenberg, S. Colle, H. G. Beyer, Solar radiation prediction based on the combination of a numerical weather prediction model and a time

series prediction model, Proc. Eurosun (ISES Europe Solar Congress), Lisbone, Portugal, 2008

[24] K. Benmouiza, A. Cheknane, Small-scale solar radiation forecasting using ARMA and nonlinear autoregressive neural network models, Theoretical and Applied Climatology, Volume 124, Issue 3, pp 945-958, May 2016.

[25] C. Gershenson, Artificial Neural Networks for beginners, https://datajobs.com/data-science-repo/Neural-Net-[Carlos-Gershenson], 2011

[26] W. McCulloch, W. Pitts, A Logical Calculus of the Ideas Immanent în Nervous Activity, Bulletin of Mathematical Biophysics, Vol. 5, pp. 115-133, 1943

[27] D. Rumelhart, J. McClelland, Parallel Distributed Processing. MIT Press, Cambridge, Mass, 1986

[28] L. Fara, A. M. Dabija, S. Fara, D. Finta, M. Iancu, M. Paulescu, Building Integrated Photovoltaics (BIPV) in Romania, Proceedings of International Congress Energy and the Environment 2008, Opatija, Croatia, October 22 - 24, 2008

[29] L. Fara, S. Fara A-M. Dabija, First results of a BIPV project in Romania, Proceedings of PL Conference, Dublin, Ireland. October, 2008

[30] https://en.wikipedia.org/wiki/Akaike_information_criterion

[31] G.E.P. Box, G.M Jenkins, Time series analysis, forecasting and control, Holden Day, San Francisco (1970)

[32] G. Reikard, Predicting solar radiation at high resolutions: A comparison of time series forecasts, Solar Energy, volume 83, issue 3, pp. 342–349, March, 2009.

[33] C. Paoli, C. Voyant, M. Muselli, M. Nivet, Forecasting of preprocessed daily solar radiation time series using neural networks, Solar Energy 84, pp. 2146–2160, 2010

[34] H. Breitkreuz, M. Schroedter-Homscheidt, T. Holzer-Popp, and S. Dech, Short-range direct and diffuse irradiance forecasts for solar energy applications based on aerosol chemical transport and numerical weather modeling, J. Appl. Meteorol. Climatol 48/9, pp. 1766–1779 2009.

[35] R. Perez, S. Kivalov, J. Schlemmer, K. Hemker, Jr., D. Renne, and T. E. Hoff, Validation of short and medium term operational solar radiation forecasts in the US, Solar Energy 84, pp. 2161–2172, 2010.

[36] E. Lorenz D., Heinemann, and A. Hammer, Short-term forecasting of solar radiation based on satellite data, in Proceedings of EUROSUN, Freiburg, Germany, 2004.

[37] D. Heinemann, E. Lorenz, and M. Girodo, Forecasting of solar radiation, in Solar Energy Resource Management for Electricity Generation from Local Level to Global Scale, edited by E. D. Dunlop, L. Wald, and M. Suri Nova Science Publishers, Hauppauge, 2006.

[38] L. A. Fernandez-Jimenez, A. Mu~noz-Jimenez, A. Falces, M. Mendoza-Villena, E. Garcia-Garrido, P. M. Lara-Santillan, E. Zorzano-Alba, and P. J. Zorzano-Santamaria, Short-term power forecasting system for photovoltaic plants, Renewable Energy 44, pp. 311–317, 2012.

[39] A. Diaconu, Contributions to the operational optimization of photovoltaic systems in applications, PhD Thesis, Polytechnic University of Bucharest, Faculty of Electronics, Telecommunications and Information Technology, Bucharest, 2017

[40] B. Bartok, Changes in solar energy availability for south-eastern Europe with respect to global warming, Phys. Chem. Earth 35, pp. 63–69, 2010

[41] S. Jerez , I. Tobin, R. Vautard, J. P. Montavez , J. Marıa, L. Romero , F. Thais, B. Bartok, O. B. Christensen, A. Colette, M. Deque, G. Nikulin, S. Kotlarski, E. van Meijgaard, C. Teichmann & M. Wild, The impact of climate change on photovoltaic power generation in Europe, Nature Communications, doi:10.1038/ncomms10014, December, 2015.

[42] http://wrdc.mgo.rssi.ru

[43] G. E. P. Box, G. M. Jenkins, and G. C. Reinsel, Time Series Analysis: Forecasting and Control, Prentice Hall, Englewood Cliffs, New Jersey, 1994.

[44] Y. Dazhi, P. Jirutitijaroen, and W. M. Walsh, Hourly solar radiation forecast including cloud cover effects using time series analysis, Solar Energy 86 (12), pp. 3531–3543, 2012.

[45] Y. Sulaiman, W. M. Hlaing, M. Wahab, Z. A. Sulaiman, Analysis of residuals in daily solar radiation time series, Renewable Energy 11(1): pp. 97-105, DOI: 10.1016/S0960-1481(96)00110-3, May, 1997

[46] O. Schäfer, J. Watson, Global Market Outlook 2015-2019, http://helapco.gr/pdf/Global_Market_Outlook_2015_-2019_lr_v23.pdf

[47] Directive 2010/31/EU of the European Parliament and of the Council of 19 May 2010 on the energy performance of buildings, 2010.

[48] Share of renewables in energy consumption in the EUrose further to16% in 2014,http://ec.europa.eu/eurostat/documents/2995521/7155577/8-10022016-AP EN.pdf/38bf822f-8adf-4e54-b9c6-87b342ead339, 30/2016, February 2016.

[49] L. Fara, A. Diaconu and F. Dragan, Trends, Challenges and Opportunities in Advanced Solar Cells Technologies and PV Market, Journal of Green Engineering, Vol. 5, pp. 157–184. doi: 10.13052/jge1904-4720.5350, 2016